Power spectra of the Sun's large-scale magnetic field during solar cycles 23 and 24

Yukun Luo (sy2130104@buaa.edu.cn), Jie Jiang (jiejiang@buaa.edu.cn), Ruihui Wang
School of Space and Environment, Beihang University, China

Astronomy for All Busan 2021

ABSTRACT

Motivation: People usually utilize Fourier decomposition of local magnetograms to derive the magnetic power spectrum and further investigate the properties of the photospheric magnetic fields, especially the small-scale field. However, the long-term evolution of the large-scale magnetic field is rarely analyzed based on the power spectrum.

Aim: We aim to investigate the power spectra using spherical harmonic decomposition of SOHO/MDI and SDO/HMI synoptic magnetograms for cycles 23 and 24.

Results: (1). The calibration factor between MDI and HMI power spectral density is spatial scale-dependent. (2). The magnetic power spectra show a distinct peak at the supergranular scale (l ≈120). (3). The power law indices for the spatial range of l =30 (AR size) and l =120 show a good anti-correlation with the amplitude of magnetic activity.

METHODS

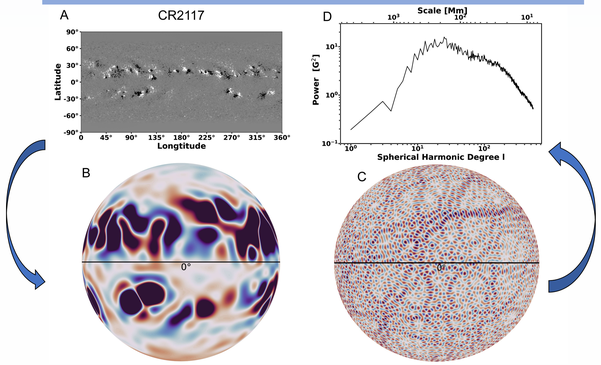

Fig. 1. Flow chart from a synoptic magnetogram to the power spectrum. (A) CR2117 synoptic magnetograms used as an example; (B) & (C) the map after spherical harmonic decomposition; (B) spherical harmonics up to the maximum degree l_{max} = 30 and projected at spherical sphere at the equator; (C) same as (B), but just for the degree of l=120; (D) the corresponding power spectrum based on the decomposition.

- Pro-processing of the synoptic magnetograms:
  HMI (MDI): 3600 points in longitude by 1440 (1080) points in sine latitude → 2880 (2160) points in longitude by 1440 (1080) points in latitude
- Spherical harmonic decomposition of the synoptic magnetograms to obtain the spherical harmonic coefficients,

$$B(\theta,\varphi)=\sum_{l=0}^{l_{max}}\sum_{m=-l}^{l}B_{l,m}Y_{l,m}(\theta,\varphi)$$

where Y_{lm} is spherical harmonics of azimuthal order m and degree l.

- Calculating the power spectra based on Parseval's theorem

RESULTS

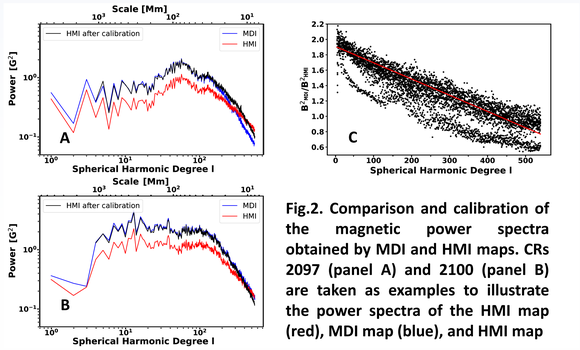

Fig.2. Comparison and calibration of the magnetic power spectra obtained by MDI and HMI maps. CRs 2097 (panel A) and 2100 (panel B) are taken as examples to illustrate the power spectra of the HMI map (red), MDI map (blue), and HMI map calibrated (black) using the red line in Panel (C) . Panel (C): spatial scale dependence of the calibration factor between MDI and HMI power spectral density. Black dots and red lines are the observations and the linear fit to the data, respectively.

- The calibration factor between MDI and HMI power spectral density (B^2_{MDI}/B^2_{HMI}) is spatial scale-dependent. The calibration function -0.0021* l +1.91 rather than 1.42^2 given by previous studies, e.g., Liu et al. (2012).
- After the spatial scale-dependent calibration, MDI and HMI show roughly the same power spectrum distributions for l in the range from l =5 to l =200.
- The spectra show a distinct peak at about l ≈120 (~ 35Mm) representing supergranules. To the best of our knowledge, this is the first report of the obvious supergranular structure based on the magnetic power spectra.

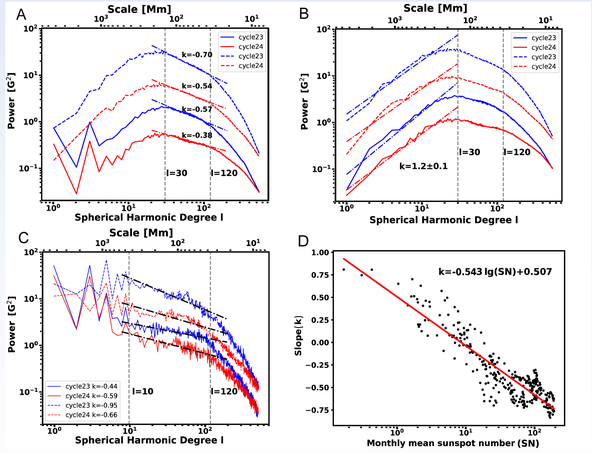

Fig.3. Magnetic power spectra for total magnetic field (panel A), for non-axisymmetric field (mode m≠0, panel B), and for axisymmetric field (mode m=0, panel C) of cycles 23 and 24. Red (blue) curves: cycle 24 (23); dotted (solid) curves: active (quieter) phase of a cycle. Panel D: Power-law indices k shown in panel A of the power spectra as a function of the corresponding sunspot number.

- Significant powers are found at two spatial scales, i.e., about l =30 (146 Mm) and l =120 (36 Mm), corresponding to the typical size of ARs and supergranulations based on the total magnetic field (Fig.3A) and the non-axisymmetric (Fig.3B) component.
- For the axisymmetric field (Fig.3C), the spectrum shows a continuous decrease from the largest scale (l ≈5) to the scale of supergranulations (l ≈120). The peak at l =5 corresponds to the structure build-up by AR emergence in the magnetic butterfly diagram. No peaks at the typical AR size (l ≈30) indicate that the AR emergence is a non-axisymmetric process.
- The power-law indices (k) for the spatial range of l =30 and l =120 show a good anti-correlation with the amplitude of magnetic activity. The function between them is k=-0.53lg(SN)+0.51.
- For the non-axisymmetric field (Fig.3B), the spectrum for the scales larger than ARs' size shows a constant power index, that is 1.2. We investigate its origin by experiments on artificially created ARs with different types of configurations in Fig.4.

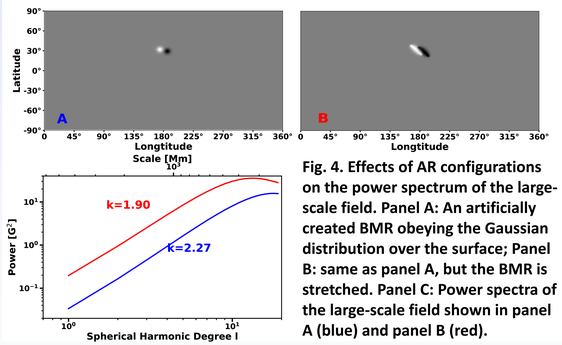

Fig. 4. Effects of AR configurations on the power spectrum of the large-scale field. Panel A: An artificially created BMR obeying the Gaussian distribution over the surface; Panel B: same as panel A, but the BMR is stretched. Panel C: Power spectra of the large-scale field shown in panel A (blue) and panel B (red).

CONCLUSIONS

- The magnetic power spectra over the broad spatial scale from about 22 Mm to the global scale for cycles 23 and 24 are derived and analyzed.
- The differences in the magnetic field strength detected by HMI and MDI data vary with spatial scales, which lead to the spatial scale-dependent calibration factors between MDI and HMI maps. After the calibration, HMI and MDI maps show consistent power spectra for the large-scale fields.
- The magnetic power spectra show a distinct peak at the supergranular scale (l ≈120), which is invisible in previous attempts using Fourier decomposition of local magnetograms.
- The slopes of the power spectra for the spatial range from l =30 (AR size) to l =120 show a good anti-correlation with the amplitude of magnetic activity.
- Axisymmetric and non-axisymmetric components of the magnetic field show different power spectra. The non-axisymmetric one shows distinct peak at about l =30. The axisymmetric one shows a continuous decrease from the large scale (l ≈5) to the scale of supergranulations.

Acknowledgements. The SDO/HMI data are courtesy of NASA and the SDO/HMI team. SOHO is a project of international cooperation between ESA and NASA. The research is supported through the National Natural Science Foundation of China (grant Nos. 12173005 and 11873023).

Reference: Liu, Y., et al. 2012, Sol Phys. 279, 295-316